

Low-Cost Fiber-Tip Fabry-Perot Interferometer and Its Application for Transverse Load Sensing

Xiaogang Jiang and Daru Chen*

Abstract—A Fabry-Perot interferometer sensor based on a fiber-tip bubble-structure micro-cavity is proposed, fabricated, and demonstrated for transverse load sensing. The micro-cavity is fabricated by using arc discharge at the end of a multimode fiber which has been processed with chemical etching. A transverse load sensitivity of 3.64 nm/N and a relative low temperature sensitivity of about 2 pm/°C are experimentally demonstrated for the proposed fiber-tip bubble-structure micro-cavity sensor. The sensor has the advantages of low-cost, ease of fabrication and compact size, which make it a promising candidate for transverse load sensing in harsh environments.

1. INTRODUCTION

As one kind of optical fiber sensors [1–5], fiber optic Fabry-Perot interferometers (FPIs), which offer the advantages of high resolution, compact structure and immunity to electromagnetic interference, play important roles in a large number of sensing applications such as refractive index [6–9], strain [10–12], temperature [13–15], pressure [16–18] and so on. Among them, the Fabry-Perot cavity which is fabricated at the fiber tip can be effectively used in space limited environment. A sealed fiber tip Fabry-Perot cavity can be fabricated by various techniques, such as sealing an etched multimode fiber [17, 18] (or hollow core fiber [16]) by silica diaphragm, splicing a silica capillary [19] (or photonic crystal fiber [20]) to a single mode fiber and then melting it to get a micro-cavity. The sensors based on the above-mentioned techniques require two or more components or materials, which may suffer thermal instability caused by the different thermal expansion coefficients and a relatively high cost at the same time.

In this paper, we propose a novel FPI manufacturing method. The manufacturing process can be divided into two steps: firstly, a chemical etching method was used to make a groove in the tip of a multimode fiber (MMF). Secondly, the etched fiber would be put into a fusion splicer and then a micro-cavity would be created in the tip of optical fiber by using arc discharge at the fiber end. To the best of our knowledge, this is the first time to fabricate a fiber tip bubble-structure micro-cavity only based on a single optical fiber without other components or materials involved. The transverse load and temperature response characteristics of the proposed sensor have been experimentally investigated.

2. SENSOR DESIGN AND FABRICATION

Chemical etching is a low-cost and easy-to-use method to make grooves in the tip of optical fibers, which has been widely used in the field of fiber sensor processing. By immersing the fiber tip in a solution of hydrofluoric acid (HF) for some time, a groove can be obtained since the chemical etching rate of the fiber core of the germanium doped silica is much faster than that of the fiber cladding of the pure silica. The scale of the groove can be changed by controlling the reaction condition, such as

Received 14 June 2014, Accepted 2 August 2014, Scheduled 23 August 2014

* Corresponding author: Daru Chen (daru@zjnu.cn).

The authors are with the Institute of Information Optics, Zhejiang Normal University, Jinhua 321004, China.

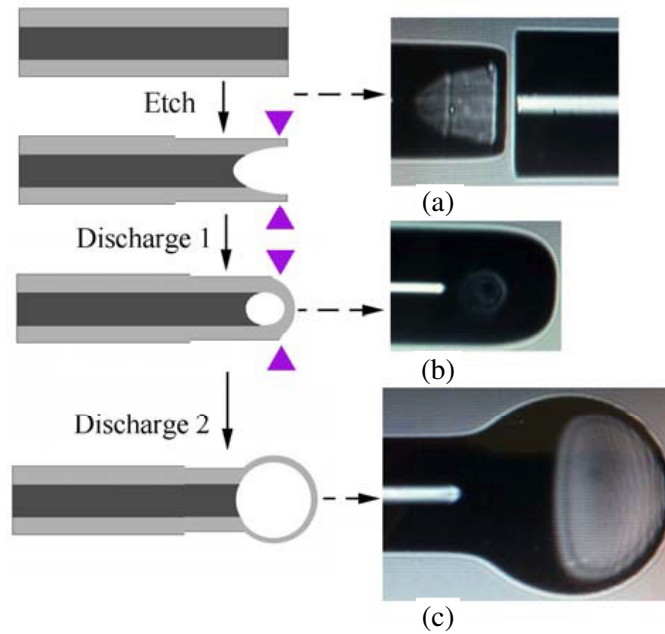


Figure 1. The schematic diagram of the fabrication process of the fiber-tip FPI. Inset (a) multimode fiber after 15 min of chemical etching compared to the fiber without any processing. (b) The sealed groove. (c) Image of micro-cavity obtained by built-in optical microscopy of the fusion splicer.

solution temperature, immersion time and acid concentration. In this paper, a MMF with $62.5\ \mu\text{m}$ core diameter was immersed in a solution of HF 40% for 15 minutes at room temperature. After cleaning, the etched fiber would be put into a fusion splicer for further operation. The schematic diagram of the fabrication process of the fiber-tip FPI is shown in Fig. 1. Inset (a) shows the image, obtained by the built-in optical microscopy of the fusion splicer, of the fiber tip after chemical etching compared to a well cleaved fiber end without any processing. The first arc discharge aims to seal the groove in the fiber end. Since the groove has a thin silica wall, the splicing parameters (arc current, arc time) should be adjusted to meet the requirement to seal the fiber tip and avoid the collapse of groove at the same time. In this step, the arc current of 5 mA and arc time of 600 ms are adopted for the fusion splicer (Jilong Optical Communication Co. Ltd. KL-300T). The sealed groove is shown in inset (b). After that, the second arc discharge with the arc current of 7 mA and the arc time of 1000 ms is applied on the sealed fiber-tip. During the discharge, the temperature reaches the softening point of silica and the air in the cavity expands simultaneously, which lead to the formation of the bubble-structure micro-cavity as shown in inset (c).

Although inset (c) in Fig. 1 shows a black part of the micro-cavity on the left, the cross-section of the bubble actually tends to be a circle, which means the black part of micro-cavity on the left is also hollow. This can be observed by using an external optical microscope, which is shown in Fig. 2(a). In this case, the real length of interference cavity is approximately $150\ \mu\text{m}$, as shown in Fig. 2(b). Here, we'd like to point out that the micro-cavity with shorter cavity length can be obtained by reducing the arc current and arc time of the second arc discharge in the fabrication process of the micro-cavity. Fig. 2(c) and Fig. 2(d) show, respectively, the micro-cavity with cavity length about $65\ \mu\text{m}$ and $100\ \mu\text{m}$. Since the reflectivity of the silica-air interface is less than 4%, the higher order reflections from these surfaces are negligible [21]. In addition, the micro-cavity has a relative thin (about $5\ \mu\text{m}$) silica wall on the right side. As a result, the sensor can be considered as a two-beam FPI with one beam from the silica-air interface on the left side of the bubble and the other from the air-silica interface on the right side of the bubble, which are indicated in Fig. 2(b).

The current intensity of the fusion splicer plays an important role in the fabrication of the micro-cavity. It should be limited in a certain range, since the sealed groove we achieved after the first discharge would be burst under higher current intensity while with no obvious effect under lower intensity. In

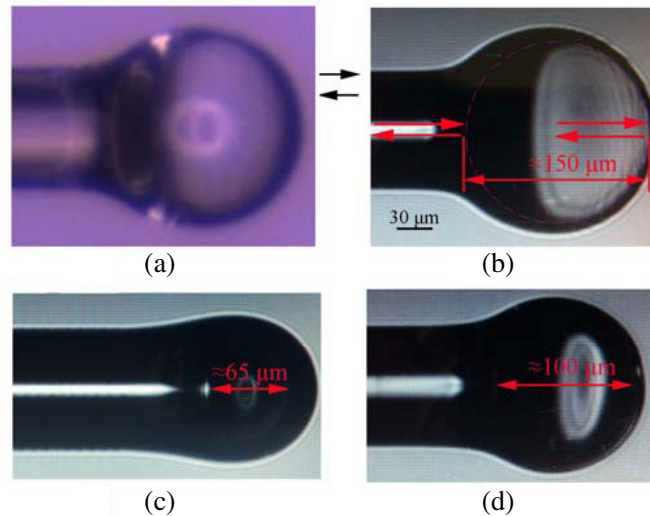


Figure 2. (a) Image of micro-cavity obtained by external optical microscope. Micro-cavity with cavity length of (b) $\sim 150 \mu\text{m}$ (c) $\sim 65 \mu\text{m}$ (d) $\sim 100 \mu\text{m}$.

our experiments, the maximum cavity length we achieved is about $150 \mu\text{m}$ and the minimum length is about $60 \mu\text{m}$. If a fusion splicer with the arc current and arc time which can be increased or decreased by smaller step is used, the cavity length of the micro-cavity can be more precisely controlled.

3. CHARACTERIZATION OF FIBER TIP MICRO-CAVITY SENSORS

Transverse load is an important detecting parameter in the field of structural health monitoring. Fiber-optic sensors based on fiber Bragg gratings [22–26] or long period gratings [27] have been reported for transverse load sensing. In this paper, we demonstrated that the transverse load sensing can be realized by using the proposed bubble-structure micro-cavity. Figure 3(a) shows the experimental setup of the transverse load sensing system for the proposed micro-cavity we mentioned in Figure 2(b). A C+L Band amplified spontaneous emission (ASE) light source which covers the wavelength range from 1520 nm to 1620 nm and an optical spectrum analyzer (OSA) with a resolution of 0.02 nm are connected to the two input ports of a 3-dB optical coupler. The fiber-tip micro-cavity sensor which is connected to the output port of the couple is fixed between two parallel copper plates. The spectrum (black line) of the ASE and the measured reflection spectrum (red line) of the micro-cavity sensor under zero pressure are shown in Figure 3(b). In our experiment, the transverse load was increasingly applied to the upper plate with a step of 0.1 N . As shown in Figure 4(a), red shift of the reflection spectrum is observed since the micro-cavity elongates longitudinally under applied transverse load. Figure 4(b) shows the shift of the dip wavelength around 1545 nm against the applied transverse load, where a linear relationship is observed. The load sensitivity, which represented by the slope of the fitted curve, is 3.64 nm/N . The spectra response to the gradually reduced transverse load also has been investigated. For a certain load value, the reflection spectrum in load step-down process is identical with that in step-up process, which means the micro-cavity has good deformation restorability.

The temperature response of the micro-cavity sensor was also investigated by inserting it inside a tube oven. The heating rate was set to be $10^\circ\text{C}/\text{min}$, and the temperature was raised up to 1000°C in steps of 250°C and maintained about 30 min at each step to make sure the temperature in the furnace has been stabilized. Fig. 5(a) shows the reflection spectra of the sensor at 20°C , 500°C , and 1000°C . Figure 5(b) shows the dip wavelength shift during the heating process. The temperature sensitivity of the sensor is about $2 \text{ pm}/^\circ\text{C}$. The relative low temperature sensitivity is determined by the characteristic of the air cavity. When the cavity sensor considered as a two-beam FPI, the thermal expansion of the cavity length play a main role in the temperature sensitivity since the thermo-optic effect of air can be negligible even for high temperature [13]. For pure silica material, the thermal expansion coefficient

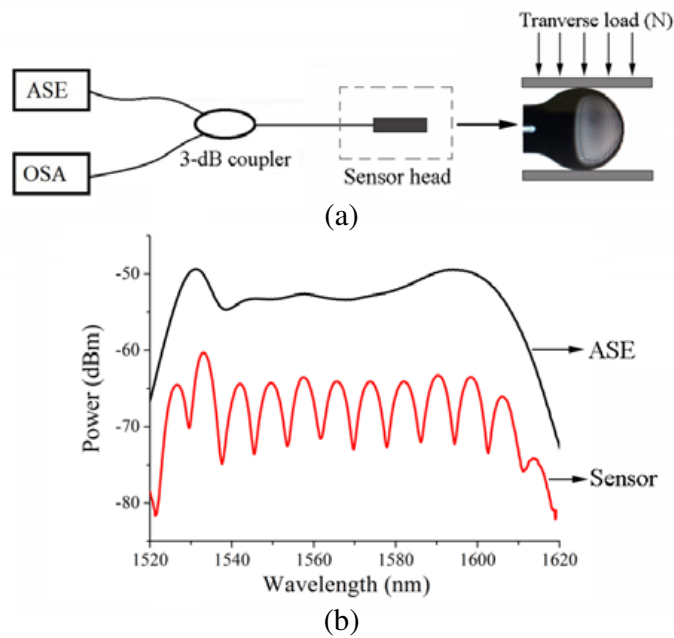


Figure 3. (a) Experimental setup of the transverse load sensing system. (b) Out spectrum of the ASE (black line) and the micro-cavity (red line).

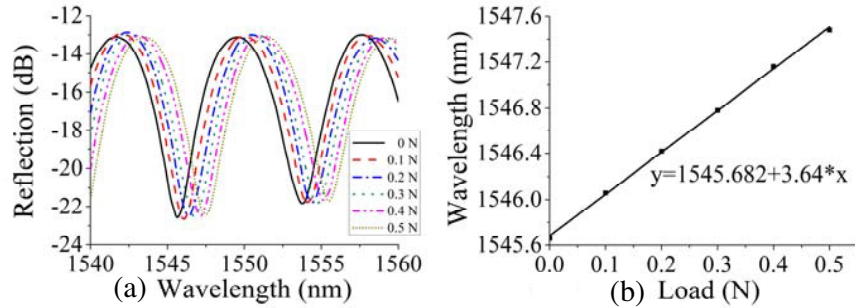


Figure 4. (a) Response of the micro-cavity sensor to transverse load. (b) Dip wavelength shift as functions of applied hydrostatic pressure.

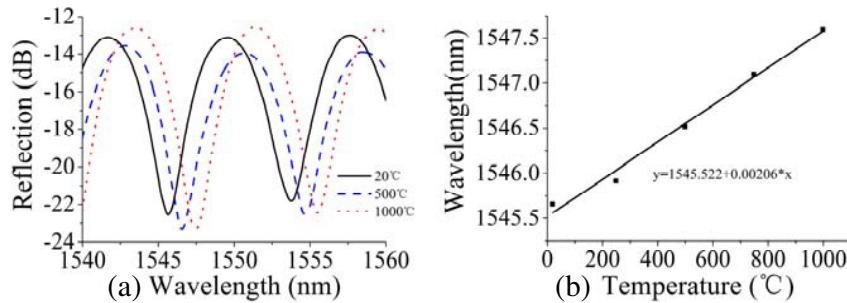


Figure 5. (a) The reflection spectra of the sensor at 20°C, 500°C, and 1000°C. (b) Dip wavelengths as functions of temperature.

$\varepsilon = 5.5 \times 10^{-7}$ [28], thus the theoretical value of temperature sensitivity is about 0.85 pm/°C. The low temperature sensitivity of sensor is preferred since it effectively reduces the cross-sensitivity to temperature in transverse load sensing application.

4. CONCLUSION

In conclusion, a compact fiber-tip bubble-structure micro-cavity sensor has been fabricated and demonstrated for transverse load sensing. The fabrication processing of the fiber-tip bubble-structure micro-cavity has been presented in details. Reflection spectra of the proposed sensor for different transverse loads and different temperatures have been investigated, which indicates it can be used as a transverse load sensor with sensitivity of 3.64 nm/N and a low temperature sensitivity of ~ 2 pm/°C. The proposed sensor has the advantages of low-cost, compact size, ease of fabrication, good mechanical strength and low cross-sensitivity to temperature.

ACKNOWLEDGMENT

This work was supported in part by Projects of Zhejiang Province (No. 2011C21038, No. 2011R10065 and No. 2010R50007), National High Technology Research and Development Program of China (863 Program) (2013AA031501), and the Program for Science and Technology Innovative Research Team in Zhejiang Normal University.

REFERENCES

1. Kersey, A. D., M. A. Davis, H. J. Patrick, M. LeBlanc, K. P. Koo, C. G. Ashins, M. A. Putnam, and E. J. Friebele, "Fiber grating sensors," *J. Lightw. Technol.*, Vol. 15, 1442–1463, 1997.
2. Culshaw, B., "Optical fiber sensor technologies: Opportunities and — perhaps — pitfalls," *J. Lightw. Technol.*, Vol. 22, 39–50, 2004.
3. Kumar, S., G. Sharma, and V. Singh, "Sensitivity modulation of surface plasmon resonance sensor configurations in optical fiber waveguide," *Progress In Electromagnetics Research Letters*, Vol. 37, 167–176, 2013.
4. Pandey, G., E. T. Thostenson, and D. Heider, "Electric time domain reflectometry sensors for non-invasive structural health monitoring of glass fiber composites," *Progress In Electromagnetics Research*, Vol. 137, 551–564, 2013.
5. Chen, D. and X. Cheng, "Hydrostatic pressure sensor based on a gold-coated fiber modal interferometer using lateral offset splicing of single mode fiber," *Progress In Electromagnetics Research*, Vol. 124, 315–329, 2012.
6. Wei, T., Y. Han, Y. Li, H. Tsai, and H. Xiao, "Temperature-insensitive miniaturized fiber inline Fabry-Perot interferometer for highly sensitive refractive index measurement," *Opt. Exp.*, Vol. 16, 5764–5769, 2008.
7. Liao, C. R., T. Y. Hu, and D. N. Wang, "Optical fiber Fabry-Perot interferometer cavity fabricated by femtosecond laser micromachining and fusion splicing for refractive index sensing," *Opt. Exp.*, Vol. 20, 22813–22818, 2012.
8. Tian, J., Y. Lu, Q. Zhang, and M. Han, "Microfluidic refractive index sensor based on an all-silica in-line Fabry-Perot interferometer fabricated with microstructured fibers," *Opt. Exp.*, Vol. 21, 6633–6639, 2013.
9. Zhao, J. R., X. G. Huang, W. X. He, and J. H. Chen, "High-resolution and temperature-insensitive fiber optic refractive index sensor based on Fresnel reflection modulated by Fabry-Pérot interference," *J. Lightw. Technol.*, Vol. 28, 2799–2803, 2010.
10. Murphy, K. A., M. F. Gunther, A. M. Vengsarkar, and R. O. Claus, "Fabry-Perot fiber-optic sensors in full-scale fatigue testing on F-15 aircraft," *Appl. Opt.*, Vol. 31, 431–433, 1992.
11. Shi, Q., F. Lv, Z. Wang, L. Jin, J. J. Hu, Z. Liu, G. Kai, and X. Dong, "Environmentally stable Fabry-Pérot-type strain sensor based on hollow-core photonic bandgap fiber," *IEEE Photon. Technol. Lett.*, Vol. 20, 237–239, 2008.
12. Liu, S., Y. Wang, C. Liao, G. Wang, Z. Li, Q. Wang, J. Zhou, K. Yang, X. Zhong, J. Zhao, and J. Tang, "High-sensitivity strain sensor based on in-fiber improved Fabry-Perot interferometer," *Opt. Lett.*, Vol. 39, 2121–2124, 2014.

13. Choi, H. Y., K. S. Park, S. J. Park, U. C. Paek, B. H. Lee, and E. S. Choi, "Miniature fiber-optic high temperature sensor based on a hybrid structured Fabry-Perot interferometer," *Opt. Lett.*, Vol. 33, 2455–2457, 2008.
14. Duan, D. W., Y. J. Rao, W. P. Wen, J. Yao, D. Wu, L. C. Xu, and T. Zhu, "In-line all-fibre Fabry-Perot interferometer high temperature sensor formed by large lateral offset splicing," *Electron. Lett.*, Vol. 47, 1702–1705, 2011.
15. Wang, J., B. Dong, E. Lally, J. Gong, M. Han, and A. Wang, "Multiplexed high temperature sensing with sapphire fiber air gap-based extrinsic Fabry-Perot interferometers," *Opt. Lett.*, Vol. 35, 619–621, 2010.
16. Wang, X., J. Xu, Y. Zhu, L. K. Cooper, and A. Wang, "All-fused-silica miniature optical fiber tip pressure sensor," *Opt. Lett.*, Vol. 31, 885–887, 2006.
17. Wang, W., N. Wu, Y. Tian, C. Niezrecki, and X. Wang, "Miniature all-silica optical fiber pressure sensor with an ultrathin uniform diaphragm," *Opt. Exp.*, Vol. 18, 9006–9014, 2010.
18. Donlagic, D. and E. Cibula, "All-fiber high-sensitivity pressure sensor with SiO₂ diaphragm," *Opt. Lett.*, Vol. 30, 2071–2073, 2005.
19. Ma, J., J. Ju, L. Jin, and W. Jin, "A compact fiber-tip micro-cavity sensor for high-pressure measurement," *IEEE Photon. Technol. Lett.*, Vol. 23, 1561–1563, 2011.
20. Jauregui-Vazquez, D., J. M. Estudillo-Ayala, A. Castillo-Guzman, R. Rojas-Laguna, R. Swlvas-Aguilar, E. Vargas-Rodrigues, J. M. Sierra-Hernandez, V. Guzman-Ramos, and A. Flores-Balderas, "Highly sensitive curvature and displacement sensing setup based on an all fiber micro Fabry-Perot interferometer," *Opt. Commun.*, Vol. 308, 289–292, 2013.
21. Villatoro, J., V. Finazzi, G. Coviello, and V. Pruneri, "Photonic-crystal-fiber-enabled micro-Fabry-Perot interferometer," *Opt. Lett.*, Vol. 34, 2441–2443, 2009.
22. LeBlanc, M., S. T. Vohra, T. E. Tsai, and E. J. Friebele, "Transverse load sensing by use of pi-phase-shifted fiber Bragg gratings," *Opt. Lett.*, Vol. 24, 1091–1093, 1999.
23. Shu, X., K. Chisholm, I. Felmeri, K. Sugden, A. Gillooly, Z. Lin, and I. Bennion, "Highly sensitive transverse load sensing with reversible sampled fiber Bragg gratings," *Appl. Phys. Lett.*, Vol. 83, 3003–3005, 2003.
24. Silva-López, M., W. MacPherson, C. Li, A. Moore, J. Barton, J. Jones, D. Zhao, L. Zhang, and I. Bennion, "Transverse load and orientation measurement with multicore fiber Bragg gratings," *Appl. Opt.*, Vol. 44, 6890–6897, 2005.
25. Jewart, C., K. P. Chen, B. McMillen, M. M. Bails, S. P. Levitan, J. Canning, and I. V. Avdeev, "Sensitivity enhancement of fiber Bragg gratings to transverse stress by using microstructural fibers," *Opt. Lett.*, Vol. 31, 2260–2262, 2006.
26. Geernaert, T., G. Luyckx, E. Voet, T. Nasilowski, K. Chah, M. Becker, H. Bartelt, W. Urbanczyk, J. Wojcik, W. De Waele, J. Degrieck, H. Terryn, F. Berghmans, and H. Thienpont, "Transversal load sensing with fiber Bragg gratings in microstructured optical fibers," *IEEE Photon. Technol. Lett.*, Vol. 21, 6–8, 2009.
27. Lium, Y., L. Zhang, and I. Bennion, "Fibre optic load sensors with high transverse strain sensitivity based on long-period gratings in B/Ge co-doped fibre," *Electron. Lett.*, Vol. 35, 661–663, 1999.
28. Braginsky, V. B., M. L. Gorodetsky, and S. P. Vyatchanin, "Thermo-refractive noise in gravitational wave antennae," *Phys. Lett. A*, Vol. 271, 303–307, 2000.